RSC Advances

PAPER

View Article Online
View Journal | View Issue

Cite this: *RSC Adv.*, 2018, **8**, 15804

Adsorption of Reactive Blue 19 from aqueous solution by chitin nanofiber-/nanowhisker-based hydrogels

Liang Liu,[a] Rong Wang,[a] Juan Yu,[a] Lijiang Hu,[c] Zhiguo Wang *[b] and Yimin Fan *[a]

Physical hydrogels prepared from partially deacetylated chitin nanofibers/nanowhiskers (DEChNs) were prepared and evaluated as a new adsorbent for Reactive Blue 19 (RB19) solutions. The effects of pH, initial dye concentration, contact time and temperature were investigated. The optimum pH value for the adsorption experiments was found to be 1.0; as pH increases, the dye adsorption capacity decreases gradually. The adsorption of RB19 onto partially deacetylated chitin nanofiber-/nanowhisker-based hydrogels (DEChNs-Gels) was relatively fast, as the equilibrium could be reached in almost 20 min. The maximum adsorption capacity was found to be 1331 mg g^{-1} at pH = 1 (degree of deacetylation (DDA) = 23%, dye concentration = 1000 mg L^{-1}), considering the practical applications, the adsorption capacity in pH = 5 (838 mg g^{-1}) was believed to have more practical significance. A pseudo-second-order kinetics model agreed very well with the experimental results. Equilibrium data also fitted well to the Freundlich adsorption isotherm model in this study. The DEChNs-Gels exhibited a high efficiency for removing RB19 from aqueous solutions as a result of their nanofibrillar network and excellent pore structure accompanied by the presence of amino groups. Even when the DDA was lowered to 15%, the adsorption capacity reached 940 mg g^{-1} due to its nanostructural assembly of nanofibers/nanowhiskers, which showed great advantages compared to highly deacetylated chitosan-based adsorbents (DDA > 70%). Considering the issue of environmental protection and adsorption efficiency, DEChNs-Gels have become a potential substitute for chitosan-based adsorbents due to the milder deacetylation process and superior performance, making this material an attractive adsorbent for textile dyes.

Received 21st February 2018
Accepted 9th April 2018

DOI: 10.1039/c8ra01563e

rsc.li/rsc-advances

1. Introduction

Environmental problems have become a global concern because of their impact on public health.[1] Among them, textile dyeing factories are a major source of environmental pollution due to the discharge of wastes to rivers.[2] Most of these dyes are highly soluble in water and can be toxic to creatures; therefore, the removal of these dyes from process or waste effluents has become environmentally important. Among several chemical and physical methods, the adsorption process is one effective technique that has been successfully employed for color removal from wastewater due to its low cost, ease of operation and greater efficiency.[3]

Many absorbents have been tested for the adsorption of dyes from aqueous solutions, such as activated carbon, chitosan, lignin, and bentonite. Among them, chitin and its derivatives have been extensively investigated as adsorbents for the removal of hazardous materials from wastewater, and their efficient adsorption potential can be attributed to a high hydrophilicity and high chemical reactivity due to a large number of functional groups.[4] However, compared to chitosan (the highly deacetylated derivative of chitin), the insolubility in general solvents of chitin due to its rigid crystalline structure greatly restricts chitin's applications.[3] Compared to the dissolution of chitin, aqueous dispersions of chitin nanofibers/nanowhiskers now can be steadily produced and have shown great potential in various applications.[5–7] In our previous study, we successfully prepared chitin nanofibers/nanowhiskers under acidic, alkali or neutral conditions depending on the manufacturing process and their characteristics. Our studies determined that the chitin nanofibers/nanowhiskers could enhance the mechanical properties, nanofibrillar network and porous structure of chitosan gel beads, which led to an improvement in the enzyme immobilization efficiency.[8] Moreover, pure chitin nanofiber-/nanowhisker-based hydrogels with

[a]Jiangsu Co-Innovation Center of Efficient Processing and Utilization of Forest Resources, Jiangsu Key Lab of Biomass-Based Green Fuel & Chemicals, College of Chemical Engineering, Nanjing Forestry University, Nanjing 210037, China. E-mail: fanyimin@njfu.edu.cn

[b]Jiangsu Provincial Key Lab of Pulp and Paper Science and Technology, College of Light Industry and food Engineering, Nanjing Forestry University, Nanjing 210037, China

[c]Zhejiang Heye Health Technology Co., LTD, Dipu Town, Anji, Zhejiang, 313300, China

different surface charges have been successfully prepared recently by a gas phase coagulation method and have been discovered to show selective absorption. Though the chitin itself possessed fewer amino groups to provide possible interactions with the dyes compared to chitosan with a high degree of deacetylation, the chitin nanofiber-/nanowhisker-based hydrogel was predicted to exhibit a distinctive performance due to its assembly of nanosized fibrils to a nanofibrillar network sustaining a unique structure. Makoto Anraku *et al.* reported that surface-deacetylated chitin nanofibers had a superior binding capacity on indole and are more effective in decreasing renal injury and oxidative stress than deacetylated chitin powder in 5/6 nephrectomized rats.[9] This proved the nanofibrillation effect of chitin with respect to its property-function. Thus, it is interesting to investigate chitin nanofiber-/nanowhisker-based hydrogels for wastewater treatment due to the following characteristics: (1) a DDA value lower than 30%, and partial deacetylation occurred on the fibril surface; (2) a relatively higher mechanical strength; (3) the assembly of chitin nanofibers/nanowhiskers forms a nanofibrillar network and porous structure.

This study reports the feasibility of hydrogels prepared from chitin nanofibers/nanowhiskers as an alternative adsorbent for RB19 removal from aqueous solution. The effects of the initial RB19 concentration, reaction temperature and pH on RB19 adsorption onto chitin nanofibers/nanowhiskers hydrogels were studied. Adsorption kinetics and isotherms were also evaluated and are discussed.

2. Experimental

2.1 Reagents and materials

Chitin with a degree of *N*-acetylation (DNAc) of 91% was purified from swimming crabs (*Portunus trituberculatus*) collected from Nantong, a seaside city in Jiangsu Province, China. Clear steps are described in detail in our previous article.[10] The textile dye Reactive Blue 19 (RB19) was purchased from Sinopharm Chemical Reagent Co., Ltd, China, and used without further purification. All other chemicals were also used without any other purification.

2.2 Preparation of chitin nanofiber-/nanowhisker-based hydrogels

To prepare chitin nanofibers/nanowhiskers, purified chitin was first deacetylated in 35% (w/w) NaOH solution at 90 °C. Then, the partially deacetylated chitin was washed with deionized water and stored at 4 °C until use. To prepare chitin nanofibers/nanowhiskers, the partially deacetylated chitin was dispersed in distilled water and drops of acetic acid were added to adjust the pH to 3 under constant stirring. The obtained suspension was homogenized and treated with ultrasonication to fabricate partially deacetylated chitin nanofibers/nanowhiskers (DEChNs). After centrifugation, an aqueous DEChN dispersion at a pH of approximately 3 was prepared.

Subsequently, the prepared DEChN dispersions were poured into a plastic beaker and placed in a larger vessel containing the appropriate ammonium hydroxide solution. After maintaining the reaction at room temperature for 12 h, all the DEChN dispersions were transformed into hydrogels. Thereafter, the hydrogels were neutralized using hydrochloric acid until the wash supernatant was neutral. The DEChN hydrogel samples are denoted as DEChNs-Gels.

2.3 Instrumental characterization

The morphology of the DEChNs was observed by transmission electron microscopy. A drop of the DEChN suspension (0.05 wt%) was deposited on an electron microscope grid coated with a carbon-reinforced formvar film and allowed to dry, followed by observation using a JEOL JEM-1400 electron microscope at an acceleration voltage of 80 kV.

The scanning electron microscopy (SEM) images of the DEChNs-Gels were obtained using a JSM 7600F (JEOL, Tokyo, Japan). Samples were coated with gold before examination. FT-IR spectra of chitin and the DEChNs-Gels were recorded from 400 to 4000 cm^{-1} at room temperature by a Nicolet Antaris FT-NIR instrument. Before the determination, hydrogels were first solvent exchanged using ethanol and *tert*-butyl alcohol. Then, these hydrogels were frozen at −78 °C and vacuum-dried for 2 days at −50 °C.

2.4 Adsorption experiments

Adsorption experiments were carried out using the batch technique with controlled temperatures and constant stirring. The effects of the intermediate pH, interaction times and adsorption isotherms were determined by solute decay in the solution supernatant.[11] To determine the optimum pH value at which the maximum adsorption was accomplished, 50 mL of dye solutions were treated with a weighed mass of hydrogel discs (corresponding to 25 mg dry weight) in 100 mL glass beakers. Then, the pH was carefully adjusted between 1 and 11 using NaOH or HCl solutions. The solutions were stirred using a magnetic stirrer at room temperature. After equilibrium was reached, the solution was filtered and the concentration of the dye in the solution was determined by means of the UV-vis spectrophotometer at $\lambda_{max} = 592$ nm.[12]

After the optimum pH value was found, the effect of the initial dye concentration was investigated. For the adsorbent dosage studies, a weighed mass of hydrogel discs (corresponding to 25 mg dry weight) was added to an aqueous solution (50 mL) of RB19, ranging from 50 to 1000 mg L^{-1} at the optimum pH investigated. After equilibrium was reached, the concentration of the dye in the solution was determined.

For all the experiments, the equilibrium adsorption capacity q_e (mg g^{-1}) was determined by the mass balance of the dye:

$$q_e = \frac{(C_o - C_e) \times V}{m} \quad (1)$$

where C_o (mg L^{-1}) is the initial concentration, C_e (mg L^{-1}) is the equilibrium concentration in the liquid phase, V (L) is the volume of the liquid phase, and m (g) is the mass of the adsorbent.

A kinetics study was performed by using different beakers containing weighed masses of hydrogel discs (corresponding to 25 mg dry weight) of DEChNs-Gels in 50 mL of the dye solution (700 mg L^{-1}). At the desired time intervals, the remaining amount of dye in the aqueous solution was determined.

3. Results and discussion

3.1 Characterization of the adsorbent

Up to now, many studies have been published concerning the adsorption of dyes onto chitin and its derivatives.[3,13–16] However, dye adsorption based on chitin nanofibers/nanowhiskers has rarely been reported. In this study, DEChNs-Gels are examined for their dye adsorption performance.

In general, chitin was difficult to convert to individual nanofibers/nanowhiskers because chitin fibrils are tightly bonded to each other through a large number of hydrogen bonds. These hydrogen bonds make chitin fibrils very difficult to individualize.[17] Therefore, pretreatment was necessary to help the fabrication of chitin nanofibers/nanowhiskers. Here, partial deacetylation was applied according to the previous articles.[8,17] The deacetylation process helped promote the cationic charged density (amino groups) on chitin. Then, the individualized chitin nanofibers/nanowhiskers with an average length of 726.55 ± 27.75 nm and width of 8.8 ± 1.25 nm were obtained by enhanced electrostatic repulsion between the cationically charged chitin fibrils in water under acidic conditions, as shown in Fig. 1a and in accordance with previous studies.[8] Nevertheless, when chitin nanofibers/nanowhiskers were used directly to adsorb dyes from their effluents, phase separation became rather difficult after the adsorption process because DEChNs were well dispersed in the acidic aqueous solutions. It was necessary to modify the physical characteristics in order to facilitate the phase separation.[15] In this study, DEChNs were transformed into hydrogels to overcome this problem.

In our previous study, we found an efficient method to prepare DEChN hydrogels.[8] When DEChN dispersions were treated with an alkaline gas phase coagulation bath, such as ammonia solution, transparent DEChN dispersions could be transformed into physical hydrogels, as shown in Fig. 1b. Slow diffusion and neutralization of acetic acid in the DEChN dispersion by evaporated ammonia was the key point in this method. This method had several advantages, such as avoiding direct contact between the dispersions and the coagulation bath, low cost, convenient operation and general applicability; in addition, any volatile alkaline coagulation bath could be applied. The formed hydrogels also showed relatively higher mechanical strength compared to other chitin-based physical hydrogels, which made them more practical. The corresponding cross-section images of DEChNs-Gels is also shown in Fig. 1b. The image indicates that the DEChNs-Gels were supported by nanostructurally assembled fiber-like textures. Rich pore structures could also be observed, and the BET surface area was determined to be approximately 125 $m^2 g^{-1}$, as we reported before. These nanofibrillar and pore structures offered advantageous conditions for the adsorption of dyes from aqueous solutions.

Fig. 1c exhibits the FTIR spectra of chitin and the DEChNs-Gels. The band at 1030 cm^{-1} was due to the C–O stretching vibration of the chitin skeleton and could be used as an internal standard, while the bands at 1560 and 1630 cm^{-1} corresponded to amide II groups. Therefore, the absorption ratios of (A1560 + A1630)/A1030 could represent the degree of *N*-deacetylation of chitin. Compared with chitin, the ratio between the absorption at 1560 + 1630 and 1030 cm^{-1} of DEChNs-Gels decreased from 1.0 to 0.89, as shown in Fig. 1c, which corresponded to the decrease in the degree of *N*-acetylation.[18] This result indicated that amino groups in DEChNs-Gels were also active even after the DEChNs transformed into hydrogels, which also corresponded to the lack of any crosslinkers in preparing these DEChNs-Gels.[16,19] Amino groups would dramatically enhance the dye adsorption capacity of absorbents, as other articles have reported.[18]

3.2 Bath dye adsorption performance using the DEChNs-Gels

3.2.1 Effect of pH on the adsorption of RB19 onto the DEChNs-Gels. The influence of pH for the adsorption of RB19 onto the DEChNs-Gels was studied, while the RB19 concentration and adsorption time were fixed at 600 mg L^{-1} and 2 h, respectively, as shown in Fig. 2a. It can be seen that the adsorption of RB19 was pH-dependent; the amount of adsorbed dye on the DEChNs-Gels decreased as the pH increased from 1 to 11. The DEChNs-Gels adsorbed a high amount of dyes at pH

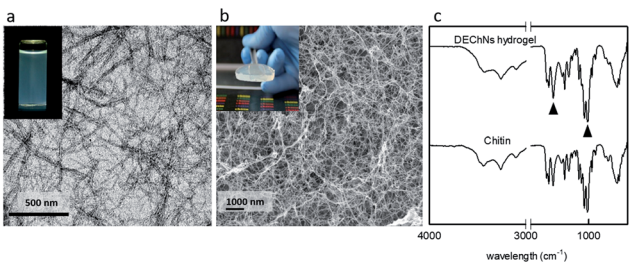

Fig. 1 Transmission electron microscopy (TEM) images of DEChNs (a), surface morphologies of the DEChNs-Gels in cross-section (b), and FT-IR spectra of chitin and the DEChNs-Gels (c).

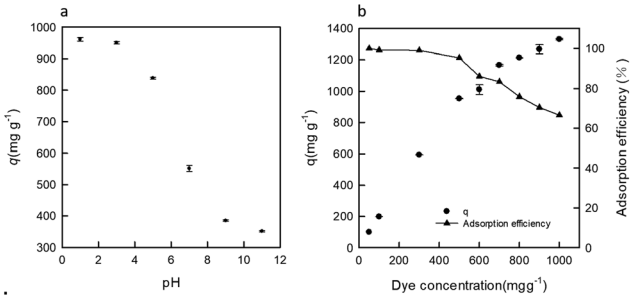

Fig. 2 The effect of pH (a) and dye concentration (b) on the RB19 adsorption onto the DEChNs-Gels at room temperature.

1.0 and pH 3.0, and the maximum uptake of RB19 occurred at pH 1.0. When the pH was increased to above 5, the adsorption of RB19 dramatically decreased. This situation can be related to the surface charge of the adsorbent and the dyes. As mentioned above, DEChNs-Gels have amino groups and showed a positively charged nature in the presence of H^+. Therefore, a strong electrostatic interaction existed between the positively charged $-NH^{3+}$ groups in the DEChNs-Gels and negatively charged $-SO_3^-$ groups in RB19. As a result, the amount of dye molecules on the DEChNs-Gels increased at lower pH values.[11]

3.2.2 Effect of initial dye concentration on the adsorption of RB19 onto the DEChNs-Gels. The removal of RB19 by the DEChNs-Gels (DDA = 23%) at various dye concentrations (ranging from 100 to 1000 mg L^{-1}) for a volume of 50 mL at a certain adsorbent dosage (corresponding to 25 mg dry weight) was also investigated. It was found that the uptake of RB19 increased, but the adsorption efficiency decreased as the dye concentration increased. When the initial dye concentrations in the solution were 50, 100 and 300 mg L^{-1}, the adsorption efficiencies reached 100, 99.12 and 99.00%, respectively; almost all of the dyes in the solution could be adsorbed. With an increase of dye concentration, the adsorption efficiency decreased gradually. The adsorption efficiencies reached 95.30, 86.02, 83.35, 75.84, 70.4 and 66.5% when the initial dye concentrations were 500, 600, 700, 800, 900 and 1000 mg L^{-1}, respectively. On the other hand, the dye adsorption capacity increased as the adsorption efficiency decreased. The dye adsorption capacities were determined to be 100, 198, 594, 953, 1011, 1167, 1213, 1267 and 1331 mg g^{-1} when the initial dye concentrations were 50, 100, 300, 500, 600, 700, 800, 900 and 1000 mg L^{-1}, respectively. The maximum dye removal was achieved at a dye concentration of 1000 mg L^{-1}, and was determined to be 1331 mg g^{-1}. This was an interesting phenomenon; it seemed that there was not a saturated adsorption capacity. This may be caused by the following hydrogel characteristics of the DEChNs-Gels: hydrogels are hydrophilic networks which can absorb large amounts of water. In our previous work, we found that the DEChNs-Gels could absorb over 250 times the weight of water compared to the dry weight of the DEChNs in the pH range below 2, which was truly a large amount of water compared to the DEChNs itself.[20] When the DEChNs-Gels were used for dye adsorption, except for the dye molecules adsorbed onto the DEChNs, the hydrogel network also sequestered a large amount of dye solution within it. When the initial dye concentration increased, the dye concentration of the restricted solution in the hydrogel network also increased, accompanied by the surface enrichment effect of the DEChNs, resulting in a continuous increase of the adsorption capacity of DEChNs-Gels. In other words, there were two ways for dye removal by the DEChNs-Gels: (1) electrostatic attraction adsorption onto the DEChNs-Gels and (2) entering the hydrophilic gels with the water, which led to the observed non-saturation of the adsorption capacity over the testing range of dye concentrations. This indicated that the hydrogel might act as an effective adsorbent.

3.2.3 Effect of DDA of chitin on the adsorption of RB19 onto the DEChNs-Gels. The most likely mechanism of the interaction between the DEChNs-Gels and dye was likely to be ionic interaction between the dye ions and the amino groups of the DEChNs-Gels, which was similar to the dye adsorption onto chitosan. In general, chitin showed a much lower dye adsorption capacity than chitosan due to the significantly fewer amino groups in chitin than in chitosan. The low number of amino groups strongly restricted the adsorption capacity of chitin for dye adsorption.[20]

In this study, we also examined the influence of the degree of deacetylation (DDA) on dye adsorption. The effect of the DDA of the DEChNs-Gels on RB19 adsorption for 25 mg dry weight of the gels and a 600 mg L^{-1} dosage of dye is shown in Fig. 3. In the preparation of the DEChNs, a suitable concentration of amino groups in the chitin was necessary for the successful fibrillation of chitin. In this study, the deacetylated chitin with DDA values of 15, 20 and 23% were prepared, from which the chitin nanofibers/nanowhiskers could be successfully obtained. At the optimized pH, the adsorption of RB19 onto these hydrogels with different DDAs was studied, while the RB19 concentration and adsorption time were fixed at 600 mg L^{-1} and 2 h. We found that the dye adsorption capacities of these prepared hydrogels reached 940, 1044 and 1147 mg g^{-1} as the DDA was 15, 20 and 23%, respectively. DEChNs-Gels showed a slightly higher dye adsorption capacity as the DDA increased. This result indicated that the increase of RB19 adsorption under acidic conditions was followed by the increase of the DDA in the DEChNs-Gels, which was similar to the dye adsorption onto chitosan. However, in this experiment, we found that even when the DDA of chitin was 15%, the as-prepared hydrogels also showed a relatively high dye adsorption capacity (940 mg g^{-1} to DDA = 15%). We believe this was a result with much more practical significance. There have been few articles concerning the RB19 adsorption onto chitin so far, but many articles reported RB19 adsorption onto chitosan (the high deacetylated derivative of chitin, normally with a degree of deacetylation higher than 70%). Among these articles, M. Hasan *et al.* found that the cross-linked chitosan/oil palm ash composite beads achieved an adsorption capacity of 400 mg g^{-1}.[21] A. Mirmohseni *et al.* reported that chitosan hollow fibers had a maximum adsorption capacity of 454.5 mg g^{-1}.[22] Nguyen Kim Nga *et al.* had prepared a chitosan film for the adsorption of RB19, and the maximum adsorption capacity was found to be 822.4 mg g^{-1}.[23]

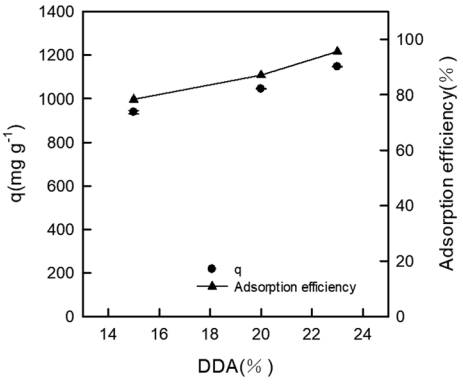

Fig. 3 The effect of the degree of deacetylation (DDA) of the DEChNs on the RB19 adsorption onto the DEChNs-Gels at room temperature.

In addition, in these studies, the chitosan must be chemically crosslinked or modified to overcome their solubility in an acidic solution, which also restricts their applications in dye adsorption. Compared to these chitosan-based materials, the DEChNs-Gels in this study retained the insoluble hydrogel nature and showed a relatively higher adsorption capacity. The higher the degree of deacetylation of the chitosan, the more demanding drastic conditions are needed to achieve it, such as more sodium hydroxide consumption or a higher reaction temperature, which results in much more environmental pollution and energy consumption. Considering the issue of environmental protection, the DEChNs-Gels with a lower degree of deacetylation might be more practical. In addition, considering the significantly fewer amino groups in the DEChNs, the DEChNs-Gels showed a much higher adsorption efficiency. This high adsorption efficiency might be attributed to the nanofibrillar network and the excellent pore structure of the DEChNs-Gels, as shown in Fig. 1b. The fibrillar network and fiber-like textured nanostructures made the circulation of the dye solution much more efficient. On the other hand, the amino groups mainly existed on the surface of the chitin nanofibers/nanowhiskers, resulting in the amino groups in the DEChNs being much more effective in the dye adsorption process, which greatly promoted the utilization efficiency of the amino groups in the DEChNs-Gels.[24,25] To conclude, dye molecules could effectively circulate in the network of the DEChNs-Gels and then be adsorbed and sequestered in the DEChNs-Gels because of the fiber-like textured nanostructures and surface amino groups in the DEChNs-Gels.

3.2.4 Adsorption kinetics. Adsorption isotherms play a very important role for understanding the adsorption mechanism.[24] In this study, different dye concentrations with the same mass of adsorbent were used to determine the adsorption mechanism. The dye adsorption capacity at a fixed dose of the DEChNs-Gels adsorbent was monitored over time, as shown in Fig. 4.

To examine the mechanism controlling the adsorption processes, such as mass transfer or chemical reactions, pseudo-first-order and pseudo-second-order kinetics models and an intraparticle diffusion model, given in eqn (2), (3) and (4), respectively, were used to test the experimental data.[16,26]

$$\log(q_e - q_t) = \log q_e - \frac{k_1}{2.303} t \quad (2)$$

$$\frac{t}{q_t} = \frac{1}{q_e^2 k_2} + \frac{t}{q_e} \quad (3)$$

$$q_t = k_i t^{1/2} + C \quad (4)$$

where q_t (mg g^{-1}) is the amount of dye uptake at time t (min); the plot of $\log(q_e - q_t)$ *versus* t gave a straight line for first-order kinetics, which allowed computation of the adsorption rate constant, k_1 (min^{-1}),[26] k_2 is the value of the pseudo-second-order rate constant [g (mg min)$^{-1}$] and k_i is the intraparticle diffusion rate constant (mg g^{-1} min$^{1/2}$); q_e is the equilibrium dye uptake (mg g^{-1}), C is the intercept (mg g^{-1}). q_e and k_1, k_2, and k_3 could be determined by plotting the experimental data according to the equations.

Fig. 4b and Table 1 show the curve-fitting plots of the pseudo-first-order and the parameters obtained for the model, respectively. Although R^2 values for the plots are in the range 0.883–0.996 (Table 2) and reasonably high in some cases, the calculated q_e values obtained from this kinetics model did not give reasonable values. This finding suggested that the sorption process did not follow the pseudo-first-order adsorption rate expression of Lagergren.[26] In contrast, all the t/q_t *versus* t gave a straight line for all the initial dye concentrations, as shown in Fig. 4c, confirming the applicability of the pseudo-second-order equation.

The coefficient values (R^2) for the pseudo-second-order kinetics equation were over 0.999, as shown in Table 2, higher than that for pseudo-first-order kinetics, suggesting the adsorption kinetics of RB19 onto the DEChNs-Gels fits the pseudo-second-order model well. The calculated q_e values also agree very well with the experimental data, as shown in Table 2.

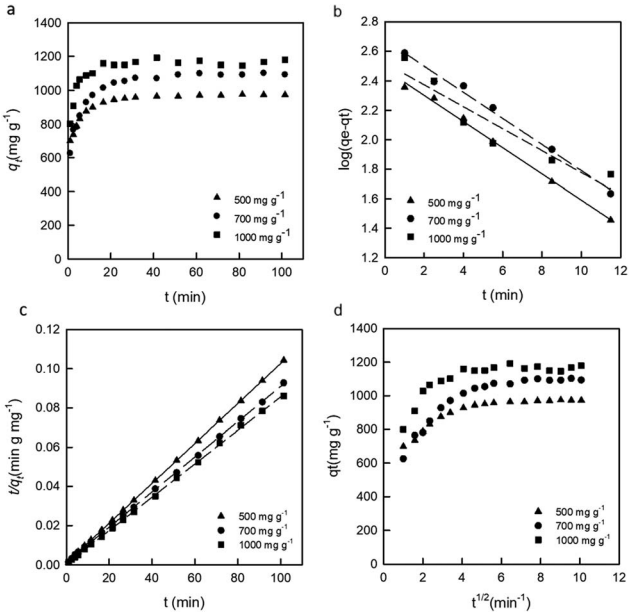

Fig. 4 The effect of dye concentration on the RB19 adsorption onto the DEChNs-Gels (a), the pseudo-first-order kinetics model curve examined (b), the pseudo-second-order kinetics model curve examined (c) and the intraparticle diffusion model examined (d) (adsorbent dose = 25 mg, solution volume = 50 mL, temperature = 20 °C and pH = 1.0).

Table 1 The pseudo-first-order kinetics parameters for the adsorption of RB19 on the DEChNs-Gels

			Pseudo-first-order	
C_o (mg L^{-1})	$q_{e\ exp}$ (mg g^{-1})	$q_{e\ cal}$ (mg g^{-1})	k_1 (min^{-1})	R^2
500	973	302	0.0958	0.996
700	1094	475	0.0974	0.986
1000	1179	333	0.1016	0.883

Table 2 The pseudo-second-order kinetics parameters for the adsorption of RB19 on the DEChNs-Gels

			Pseudo-second-order	
C_o (mg L^{-1})	$q_{e\ exp}$ (mg g^{-1})	$q_{e\ cal}$ (mg g^{-1})	k_1 (g (mg min)$^{-1}$)	R^2
500	973	983	0.001156	0.999
700	1094	1109	0.00081	0.999
1000	1179	1176	0.00165	0.999

The finding further proved the adsorption system obeyed the pseudo-second-order kinetics model for the entire sorption period and thus supported that the adsorption process was controlled not by diffusion but by chemisorption. The adsorption of the dye took place probably *via* surface exchange reactions until the surface functional sites were fully occupied, and thereafter the dye molecules diffuse into the inner structure for further interactions and/or reactions (such as an inclusion complex, hydrogen bonding, hydrophobic interactions).[26]

Adsorption was a multi-step process involving transport of the solute molecules from the aqueous phase to the surface of the solid particles followed by diffusion of the solute molecules into the pore interiors. In a batch system with rapid stirring, there was a possibility that the transport of adsorbate from the solution into the pores (bulk) of the adsorbent was the rate controlling step. This possibility was tested in terms of a graphical relationship between the amount of dye adsorbed and the square root of time. The root time dependence described by Weber and Morris is expressed by eqn (4).[27] So, the kinetics results could be used to determine if particle diffusion was the rate-limiting step for dye adsorption.[26]

Fig. 4d shows the amount of dye adsorbed *versus* $t^{1/2}$ for the intraparticle transport of RB19 onto DEChNs-Gels at different initial dye concentrations. The curves present a multilinearity, which indicates that two or more steps occurred in the process, and the sorption process tended to be followed by three phases: the first initial portion of the plot indicates surface adsorption and rapid external diffusion, while the second linear portion is the gradual adsorption stage where the intra-particle diffusion is rate controlled. The third plateau is the final equilibrium stage, where the intra-particle diffusion started to slow down due to the low solute concentration in solution. The second step between the initial rapid external diffusion stage and the equilibrium stage was chosen to characterize the rate parameter corresponding to the intraparticle diffusion. The calculated k_i values for each initial concentration are given in Table 3.

When dye concentration was fixed at 500 or 700 mg L^{-1}, R^2 values for the diffusion model were found to be 0.901 and 0.881, respectively. This indicated that the adsorption process could be followed by an intra-particle diffusion after around 10 min. However, the results did not pass through the origin (the plots had intercepts in the range 909–1105 mg g^{-1}), indicating that intraparticle diffusion was involved in the sorption process but it was not the only rate-limiting mechanism.[26] In contrast, the adsorption curve under a dye concentration of 1000 mg L^{-1} presented really low R^2 values of 0.371. This might be due to the unstable desorption at high substrate concentration, which leads to the disorder of the adsorption curve. In summary, the pseudo-second-order model was the best one in describing the adsorption kinetics of the BR10 onto DEChNs-Gels.

The effect of temperature was another important factor help to export important conclusions about the thermodynamic properties of the dye-adsorbent system.[19] Therefore, to further analyze the adsorption process, a brief thermodynamic analysis was carried out, as shown in Fig. 5. The pseudo-second-order kinetics model given in eqn (3) was also used to test the experimental data. The result is listed in Table 4. As shown in Fig. 5, the q_e increased rapidly in the initial stages with increasing contact time. As the temperature increased, the q_e increased slightly faster at the first stage (<10 min), which indicated that the adsorption of RB19 onto the DEChNs-Gels was an endothermic process.[28] Then, the q_e gradually increased until equilibrium. Table 2 shows that the coefficient values (R^2) for each adsorption system were over 0.999, proving again that the adsorption kinetics of RB19 onto DEChNs were chemisorption-controlled. The results also showed that the dye adsorption of RB19 onto the DEChNs-Gels was a fast process and could reach equilibrium in 20 min. This was believed resulting from the fiber-like textured nanostructures and surface amino groups in the DEChNs-Gels.

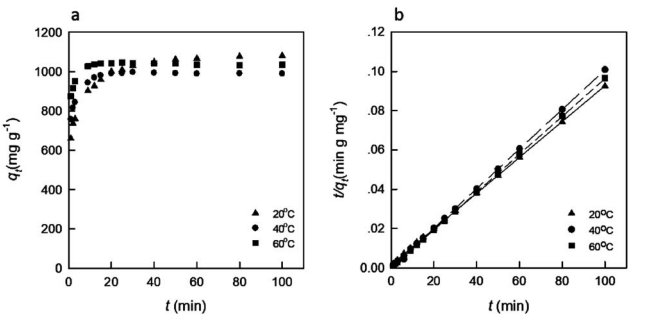

Fig. 5 The effect of temperature on the RB19 adsorption onto the DEChNs-Gels (a) and the pseudo-second-order kinetics model curve examined (b) (adsorbent dose = 25 mg, solution volume = 50 mL, dye concentration = 700 mg L^{-1} and pH = 1).

Table 3 Intraparticle diffusion parameters for the adsorption of RB19 on the DEChNs-Gels at various initial dye concentrations

C_o (mg L^{-1})	k_i (mg g^{-1} $min^{1/2}$)	C (mg g^{-1})	R^2
500	8.1434	909	0.901
700	17.1267	968	0.881
1000	10.2012	1105	0.371

Table 4 The pseudo-second-order kinetics parameters for the adsorption of BR19 onto the DEChNs-Gels

Temperature (°C)	k_2 (g (mg min)$^{-1}$)	q_e (mg g^{-1})	R^2
20	0.00054	1098	0.999
40	−0.01189	987	0.999
60	0.00330	1037	0.999

3.2.5 Equilibrium isotherms. Adsorption isotherms indicated the relationship between the mass of dye adsorbed at constant temperature per unit mass of the adsorbent and the liquid phase dye concentration.[1] Fig. 6 shows the adsorption isotherm, the relationship between the amount of adsorbed dye per unit mass of adsorbent (q_e) and the remaining dye concentration in the aqueous phase (C_e). The equilibrium data were analyzed according to the Langmuir and Freundlich adsorption isotherms, respectively. Of these, the Langmuir adsorption isotherm assumed a monolayer adsorption of the adsorbate over a homogeneous adsorbent surface where each molecule adsorbed onto its surface with an equal adsorption activation energy. For the Langmuir adsorption isotherm, no adsorbate migration occurred after adsorption. In contrast, the Freundlich adsorption isotherm describes reversible adsorption and was not restricted to the formation of a monolayer, and it was applicable to adsorption on heterogeneous surfaces with interactions between the adsorbed molecules.

The Langmuir adsorption isotherm in the linear form was expressed as the following equation:

$$\frac{C_e}{q_e} = \frac{C_e}{q_m} + \frac{1}{bq_m} \quad (5)$$

where C_e is the equilibrium dye concentration (mg L^{-1}), q_e is the equilibrium amount of adsorbed dye per unit weight of adsorbent (mg g^{-1}), q_m is the maximum amount of adsorbed dye per unit weight of adsorbent to form a complete monolayer coverage (mg g^{-1}) and b is the Langmuir adsorption constant (L mg^{-1}).

The Freundlich isotherm was expressed as the following equation:

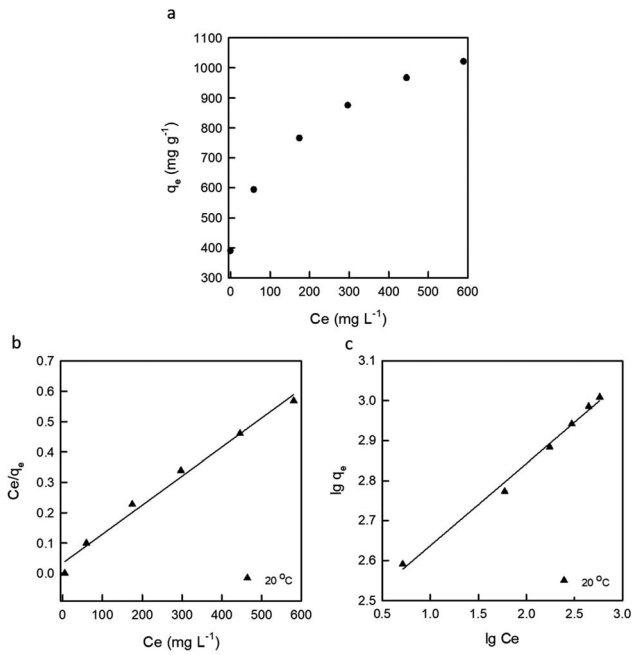

Fig. 6 Isotherm plots (a), Langmuir isotherm (b) and Freundlich isotherm (c) of RB19 adsorption onto the DEChNs-Gels (adsorbent dose = 25 mg, solution volume = 50 mL and solution temperature = 20 °C).

$$\lg q_e = \lg k + \frac{1}{n} \lg C_e \quad (6)$$

where k is the Freundlich adsorption constant, which roughly indicates the adsorption capacity of the adsorbent (mg g^{-1}), and n is the Freundlich exponent which relates the adsorption intensity.[16] The plots of C_e/q_e *versus* C_e and lg q_e *versus* lg C_e are shown in Fig. 6. The model parameters and correlation factor (R^2) are listed in Table 5.

From the value of the correlation coefficient (R^2) in Table 5, it was clear that the adsorption curves fitted better to the Freundlich isotherm than the Langmuir isotherm, indicating that the adsorption of RB19 on the DEChNs-Gels was multilayer adsorption. In addition, the maximum dye uptake of the given adsorbent (1331 mg g^{-1}) in this article indicated that the DEChNs-Gels were efficient for the removal of RB19 from aqueous solutions. This value was also comparable to the sorption capacities of some other adsorbent materials for RB19 (Table 6). Considering the similar structure and the fact that DEChNs showed about a 62% higher adsorption capacity compared to the chitosan film and only 11% lower compared to poly(methyl methacrylate) grafted chitosan adsorption capacity. The easier preparation process, much milder deacetylation conditions and relatively high adsorption capacity made DEChNs become potential substitute for chitosan-based adsorbents.

3.2.6 Desorption analysis. Desorption was an important factor for absorbents. Here we also investigated the desorption property of DEChNs-Gels. After DEChNs-Gels reached an adsorption equilibrium under optimum conditions (adsorbent dose = 25 mg, solution volume = 50 mL, dye concentration = 700 mg L^{-1} and pH = 1), the dye adsorbed DEChNs-Gels were first thoroughly washed using distilled water to remove the remaining residual dye solution. Then the particle like adsorbent was suspended in distilled water (50 mL) and HCl or NaOH was used for adjusting the pH to 1, 3, 5, 7, 9 and 11. After stirring for 2 hours, the concentration of dye in the solution was determined and the desorption efficiency was calculated as eqn (7).

$$\text{Desorption percentage}\% = \frac{C_b \times V_b}{q_e \times m} \times 100\% \quad (7)$$

where C_b is the dye concentration after desorption, V_b is the solution volume, q_e is the equilibrium adsorption of dyes, and m is the mass content of the DEChNs-Gels for the desorption experiments.

As shown in Fig. 7, the desorption percentage for RB19 was pH-dependent and achieved the highest value (about 9.02%) at pH 11. When pH decreased, the desorption values of RB19 were decreased clearly, lower than 1.5% when the pH was lower than

Table 5 The pseudo-second-order kinetics parameters for the adsorption of BR 19 on the DEChNs-Gels

Langmuir isotherm			Freundlich isotherm		
q_m (mg g^{-1})	b (L mg^{-1})	R^2	$1/n$	k (mg g^{-1})	R^2
1046	0.0281	0.986	0.2058	269.77	0.993

Table 6 Reports the maximum adsorption capacities in the literature for Reactive Blue 19 obtained on low-cost adsorbents

Adsorbent	q_{max} (mg g^{-1})	Reference
DEChNs-Gels	1331	
Poly(methyl methacrylate) grafted chitosan	1498	16
Chitosan films	822.4	23
Mesoporous carbon	733	29
(DTMA) bromide modified bentonite	206.58	30
Magnesium oxide	250	31
Lignocellulosic waste	75.19	32

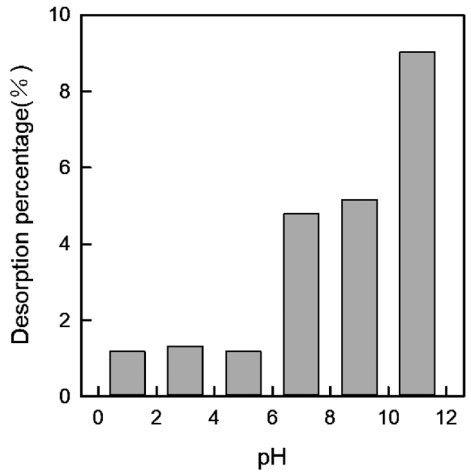

Fig. 7 Desorption of RB19 from DEChNs-Gels under various pH condition (pH = 1, 3, 5, 7, 9, 11) (adsorbent dose = 25 mg, solution volume = 50 mL).

6 after reaching the maximum value at pH 11. This phenomenon also agreed with the RB19 adsorption onto chitosan film.[23] However, here DEChNs-Gels exhibited a much lower desorption efficiency compared to chitosan film (about 72% at pH 11). Fewer but more active surface amino groups in DEChNs-Gels might be the reason for this lower desorption efficiency but stronger bonding between RB19 and DEChNs-Gels.

4. Conclusions

This study shows that the DEChNs-Gels acted as an effective adsorbent for the removal of RB19 dye from aqueous solution. The amount of dye adsorption was dependent on pH, adsorbent dosage, temperature, the degree of deacetylation of chitin and contact time. The adsorbent was the most effective at pH = 1.0. The adsorption of RB19 onto the DEChNs-Gels increased with an increase in the dosage and the degree of deacetylation of chitin. The maximum adsorption capacity was found to be 1331 mg g^{-1} at pH = 1.0 and the DDA = 23% in the testing range. In contrast, when the DDA was 15%, the adsorption capacity also reached 940 mg g^{-1}, which showed a great advantage compared to chitosan-based adsorbents considering the issues of environmental protection and adsorption efficiency. The dye adsorption of RB19 onto the DEChNs-Gels was a fast process and could reach equilibrium in 20 min. As the temperature increased, DEChNs-Gels showed a faster adsorption behavior in the first stage, but there was no significant influence on the adsorption capacity. The pseudo-second-order kinetics model agreed very well with the experimental results. Equilibrium data also fitted well to the Freundlich adsorption isotherm model in this study. The results indicate that the partially deacetylated chitin nanofiber-/nanowhisker-based hydrogel is an attractive adsorbent for the adsorption of textile dyes and could become a potential substitute for chitosan-based adsorbents.

Conflicts of interest

There are no conflicts of interest to declare.

Acknowledgements

This research was supported by the National Natural Science Foundation of China (31100426), the Jiangsu Provincial Natural Science Foundation of China (BK20170924), the Doctorate Fellowship Foundation of Nanjing Forestry University, and the Priority Academic Program Development of Jiangsu Higher Education Institutions (PAPD).

References

1 H. Tang, W. Zhou and L. Zhang, *J. Hazard. Mater.*, 2012, **209–210**, 218–225.
2 A. B. Albadarin, M. N. Collins, M. Naushad, S. Shirazian, G. Walker and C. Mangwandi, *Chem. Eng. J.*, 2017, **307**, 264–272.
3 M. S. Chiou, P. Y. Ho and H. Y. Li, *Dyes Pigm.*, 2004, **60**, 69–84.
4 R. N. Tharanathan and F. S. Kittur, *Crit. Rev. Food Sci. Nutr.*, 2003, **43**, 61–87.
5 R. Dolphen and P. Thiravetyan, *Chem. Eng. J.*, 2011, **166**, 890–895.
6 C. Zhong, A. Kapetanovic, Y. Deng and M. Rolandi, *Adv. Mater.*, 2011, **23**, 4776–4781.
7 S. Ifuku, in *Handbook of Polymer Nanocomposites. Processing, Performance and Application: Volume C: Polymer Nanocomposites of Cellulose Nanoparticles*, 2015, pp. 165–178.
8 L. Liu, R. Wang, J. Yu, J. Jiang, K. Zheng, L. Hu, Z. Wang and Y. Fan, *Biomacromolecules*, 2016, **17**, 3773–3781.
9 M. Anraku, R. Tabuchi, S. Ifuku, T. Nagae, D. Iohara, H. Tomida, K. Uekama, T. Maruyama, S. Miyamura, F. Hirayama and M. Otagiri, *Carbohydr. Polym.*, 2017, **161**, 21–25.
10 L. Liu, H. Lv, J. Jiang, K. Zheng, W. Ye, Z. Wang and Y. Fan, *RSC Adv.*, 2015, **5**, 93331–93336.
11 J. A. González, M. E. Villanueva, L. L. Piehl and G. J. Copello, *Chem. Eng. J.*, 2015, **280**, 41–48.
12 Ö. Gök, A. S. Özcan and A. Özcan, *Appl. Surf. Sci.*, 2010, **256**, 5439–5443.
13 W. Ma, F. Q. Ya, M. Han and R. Wang, *J. Hazard. Mater.*, 2007, **143**, 296–302.

14 L. Wang, J. Zhang and A. Wang, *Desalination*, 2011, **266**, 33–39.
15 T. V. Rêgo, T. R. S. Cadaval, G. L. Dotto and L. A. A. Pinto, *J. Colloid Interface Sci.*, 2013, **411**, 27–33.
16 X. Jiang, Y. Sun, L. Liu, S. Wang and X. Tian, *Chem. Eng. J.*, 2014, **235**, 151–157.
17 Y. Fan, T. Saito and A. Isogai, *Carbohydr. Polym.*, 2010, **79**, 1046–1051.
18 Y. Shigemasa, H. Matsuura, H. Sashiwa and H. Saimoto, *Int. J. Biol. Macromol.*, 1996, **18**, 237–242.
19 G. Z. Kyzas, N. K. Lazaridis and M. Kostoglou, *Chem. Eng. J.*, 2014, **248**, 327–336.
20 N. Sakkayawong, P. Thiravetyan and W. Nakbanpote, *J. Colloid Interface Sci.*, 2005, **286**, 36–42.
21 M. Hasan, A. L. Ahmad and B. H. Hameed, *Chem. Eng. J.*, 2008, **136**, 164–172.
22 A. Mirmohseni, M. S. Seyed Dorraji, A. Figoli and F. Tasselli, *Bioresour. Technol.*, 2012, **121**, 212–220.
23 N. K. Nga, H. D. Chinh, P. T. T. Hong and T. Q. Huy, *J. Polym. Environ.*, 2016, 1–10.
24 M. S. El-Geundi, *Water Res.*, 1991, **25**, 271–273.
25 K. S. Low and C. K. Lee, *Bioresour. Technol.*, 1997, **61**, 121–125.
26 G. Crini, H. N. Peindy, F. Gimbert and C. Robert, *Sep. Purif. Technol.*, 2007, **53**, 97–110.
27 W. J. Weber and J. C. Morris, *J. Sanit. Eng. Div., Am. Soc. Civ. Eng.*, 1963, **89**, 31–60.
28 Y. S. Al-Degs, M. I. El-Barghouthi, A. H. El-Sheikh and G. M. Walker, *Dyes Pigm.*, 2008, **77**, 16–23.
29 G. P. Hao, W. C. Li, S. Wang, S. Zhang and A. H. Lu, *Carbon*, 2010, **48**, 3330–3339.
30 A. Özcan, Ç. Ömeroğlu, Y. Erdoğan and A. S. Özcan, *J. Hazard. Mater.*, 2007, **140**, 173–179.
31 N. K. Nga, P. T. T. Hong, T. D. Lam and T. Q. Huy, *J. Colloid Interface Sci.*, 2013, **398**, 210–216.
32 M. Asgher and H. N. Bhatti, *Can. J. Chem. Eng.*, 2012, **90**, 412–419.